Available online at www.sciencedirect.com

SCIENCE DIRECT®

Journal of the European Ceramic Society 25 (2005) 957–962

www.elsevier.com/locate/jeurceramsoc

# Effect of $V_2O_5$ on sintering behaviour, microstructure and dielectric properties of textured $Sr_{0.4}Ba_{0.6}Nb_2O_6$ ceramics

Q. W. Huang [a,*], L. H. Zhu [b], J. Xu [b], P. L. Wang [a], H. Gu [a], Y. B. Cheng [c]

[a] *The State Key Laboratory of High Performance Ceramics and Superfine Microstructure, Shanghai Institute of Ceramics, Chinese Academy of Sciences, Shanghai 200050, China*

[b] *School of Materials Science and Engineering, Shanghai University, Shanghai 200072, China*

[c] *School of Physics and Materials Engineering, Monash University, Clayton, Vic. 3800, Australia*

Received 30 August 2003; received in revised form 11 December 2003; accepted 20 December 2003

Available online 24 June 2004

**Abstract**

The acicular $Sr_{0.39}Ba_{0.48}K_{0.32}Nb_2O_6$ single crystal particles were first prepared by the reaction of $SrCO_3$, $BaCO_3$ and $Nb_2O_5$ in molten $K_2SO_4$ at 1300 °C for 3 h. By using these single crystal particles as seeds and $V_2O_5$ as additives, textured $Sr_{0.4}Ba_{0.6}Nb_2O_6$ (SBN40) ceramics were obtained. The effect of $V_2O_5$ on sintering behaviour, microstructure and dielectric properties of textured SBN40 ceramics was investigated. The experimental results show that the addition of $V_2O_5$ can accelerate the densification rate of the material and encourage the texture of SBN40 ceramics, which further improves the anisotropy in dielectric properties between different directions of textured SBN40 ceramics.



*Keywords:* $(Sr,Ba)Nb_2O_6$; Additives; Sintering; Microstructure; Dielectric properties

## 1. Introduction

The growth of strontium barium niobate ($Sr_xBa_{1-x}Nb_2O_6$, $0.25 \leq x \leq 0.75$ abbreviated as SBN) single crystals with different compositions, and the effect of composition on properties, is widely studied because of its immense importance in many technological applications such as electro-optic,[1–3] pyro-electric,[4,5] piezoelectric,[6–8] and photo-refractive devices.[9–11] But the high cost and difficult fabrication of SBN single crystals have laid restrictions on their applications. In recent years, SBN ceramics have gained increasing attention since they are easier and cheaper to fabricate into large sizes and complex shapes. However, the randomly oriented grains often impair the electrical properties of SBN ceramics. Recently, some studies have shown that textured SBN ceramics have excellent electrical properties, which opens up one effective way to improve the electrical properties of SBN ceramics.[8,12]

Templated grain growth (TGG) is so far considered to be the most effective method to obtain textured ceramics. The process involves orienting anistropically-shaped template particles in a dense, fine-grained matrix. Template particles must be large and anisometric in shape, so that they can be oriented during forming, and grow preferentially during heating. The final texture in the microstructure is dependent strongly on the number of template particles, the relative size of matrix and template particles and sintering additives. Duran et al.[12] studied the microstructure and electrical properties of textured $Sr_{0.53}Ba_{0.47}Nb_2O_6$ ceramics, which were fabricated using $KSr_2Nb_5O_{15}$ (KSN) particles as template and $V_2O_5$ as additive, but the effect of $V_2O_5$ additive on sintering behaviour, texture development and dielectric properties is not clear. In addition, the template particles $KSr_2Nb_5O_{15}$ contained minor amounts of impurities $SrNb_2O_6$ and $Sr_2Nb_2O_7$, which made it difficult to design the composition of SBN ceramics properly. In this paper, pure, acicular strontium barium potassium niobate particles were first synthesised by means of molten salt synthesis (MSS). By using these acicular particles as seeds, the effect of $V_2O_5$ additives on sintering behaviour, texture development and dielectric properties of textured $Sr_{0.4}Ba_{0.6}Nb_2O_6$ ceramics was investigated.

* Corresponding author.
*E-mail address:* huangqw@mail.slc.ac.cn (Q.W. Huang).

0955-2219/$ – see front matter © 2004 Elsevier Ltd. All rights reserved.
doi:10.1016/j.jeurceramsoc.2003.12.027

## 2. Experimental details

Reagent grade oxides, $SrCO_3$ (purity: 99.95%), $BaCO_3$ (purity: 99.95%), $Nb_2O_5$ (Purity: 99.99%) and $K_2SO_4$ (purity: 99.95%) were used as starting powders. Acicular $Sr_{0.4}Ba_{0.6}Nb_2O_6$ template particles were prepared via MSS from $SrCO_3$, $BaCO_3$ and $Nb_2O_5$, in which $K_2SO_4$ was added at a weight ratio of 1:1. The mixture was sealed in an alumina crucible and then heated at 1300 °C for 3 h in air. On the completion of reaction, flux salt was removed from the powder particles by repeated washing with hot deionised water until no chloride ions were detected by silver nitrate.

The matrix powders $SrNb_2O_6$ (SN) and $BaNb_2O_6$ (BN), used to synthesise textured $Sr_{0.4}Ba_{0.6}Nb_2O_6$ ceramics, were prepared separately by ball-milling $SrCO_3$ or $BaCO_3$ and $Nb_2O_5$ for 24 h in ethanol. Then the dried powders were calcined at 950 °C for 3 h. After appropriate amounts of SN, BN according to $Sr_{0.4}Ba_{0.6}Nb_2O_6$ composition and 0.5 wt.% $V_2O_5$ additive were mixed with a solvent (60 vol.% toluene–40% ethanol) and milled for 24 h, 10 wt.% template particles, poly(vinyl butyral) (binder), triethanolamine (modifier) and diethyl-*o*-phthate (plasticiser) were added and mixed for 6 h. The slurry consisting of 10 wt.% template particles was tape-casted to obtain some 0.1 mm-thick sheets, which were cut, laminated and pressed at 100 MPa to form green compacts (6 mm × 6 mm × 12 mm). The green compacts were heated at 600 °C for 2 h to remove organic ingredients and then isostatically pressed at 200 MPa at room temperature. Finally the specimens were sintered between 1100 and 1425 °C in air at a heating rate of 4 °C/min for 3 h.

Randomly oriented specimens were prepared according to the conventional method. The $Sr_{0.4}Ba_{0.6}Nb_2O_6$ powders synthesised by the reaction of $SrCO_3$, $BaCO_3$ and $Nb_2O_5$ at 1100 °C for 3 h were mixed, uniaxially pressed at 100 MPa and further isostatically pressed at 200 MPa and sintered at 1300 °C for 3 h.

The bulk density of samples was measured in water by Archimede's principle. The texture, perpendicular to tape casting direction, as well as phase assembly, was determined using X-ray diffractometry (XRD) with Cu Kα. The specimens with or without grain orientation were polished and thermally etched for microstructure observation which was carried out by scanning electron microscope (SEM, Model HITACHI 270) with an energy dispersive X-ray spectrometer (EDS). The specimens were electroded by silver paste. The dielectric constant and dielectric loss at 1 kHz were measured on unpoled samples from room temperature to 250 °C using a HP4192A impedance analyzer.

## 3. Results and discussion

### 3.1. Synthesis of acicular template particles

It is worth noticing that the synthesised product from $SrCO_3$, $BaCO_3$, and $Nb_2O_5$ in molten $K_2SO_4$ consists of the expected tetragonal tungsten bronze phase and minor amount of $BaSO_4$, which can be easily removed by the conventional sedimentation method due to the considerable difference in particle size. An XRD pattern of the powder synthesised via MSS at 1300 °C is shown in Fig. 1. It can be seen that the synthesised powder from which $BaSO_4$ has been removed is composed of single tetragonal tungsten bronze phase. In comparison with $Sr_{0.4}Ba_{0.6}Nb_2O_6$ prepared by the conventional mixed-oxide method (CMO) ($a = 1.24731$ nm, $c = 0.396653$ nm),[13] the unit-cell dimensions of SBN synthesised by MSS are larger (see Table 1). EDS analysis shows the seed particles contain a certain amount of K in addition to Sr, Ba, Nb, and O (see Table 1), indicating that K in $K_2SO_4$ can substitute for Sr, Ba during the formation of $Sr_{0.4}Ba_{0.6}Nb_2O_6$ seed particles in the form of $Sr_{0.39}Ba_{0.48}K_{0.33}Nb_2O_6$.

SBN has a tungsten bronze structure with a unit-cell formula of $(A1)_4(A2)_2C_4B_{10}O_{30}$,[14] in which the A1, A2, C and B cations are in the 15-, 12-, 9- and 6-fold-coodinated sites, respectively. The $Ba^{2+}$ and $Sr^{2+}$ occupy five of the six ($A_1$, $A_2$)-sites. In the sample fired in KCl flux, two potassium ions substitute for one strontium or barium ions

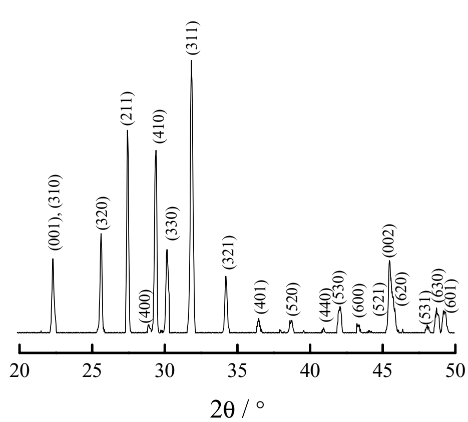


Fig. 1. XRD pattern of the powder synthesised via MSS at 1300 °C.

Table 1
Lattice parameters, chemical compositions and morphology characterisation of the synthesised seed particles

| Lattice parameters | | | Chemical compositions (at.%) | | | | | Morphology characterisation | |
|---|---|---|---|---|---|---|---|---|---|
| $a = b$ (nm) | $c$ (nm) | Volume ($nm^3$) | K | Sr | Ba | Nb | O | Length (μm) | Aspect ratio |
| 1.2519(2) | 0.3980(1) | 0.6237 | 3.32 | 3.90 | 4.78 | 22.01 | 65.99 | 4–43 | 4–22 |

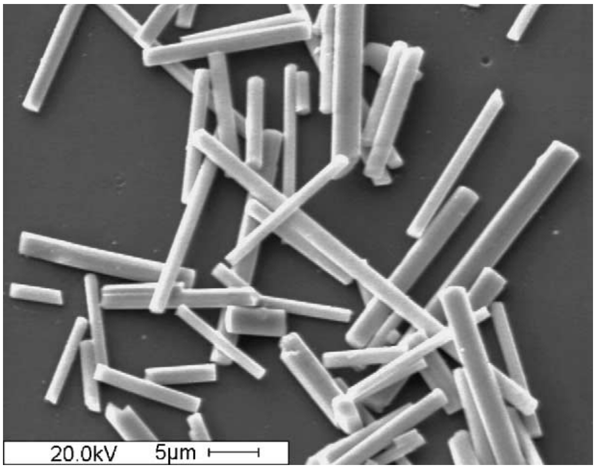


Fig. 2. SEM micrograph of acicular $Sr_{0.4}Ba_{0.6}Nb_2O_6$ template particles prepared via MSS.

in $Sr_{0.4}Ba_{0.6}Nb_2O_6$. Potassium ions are considered to distribute in —$A_1$ and $A_2$—interstitial sites in a random manner. Considering that the ionic radius of potassium (1.51 Å) is larger than the barium ion (1.42 Å) and that there are more cations in the unit cell, it can be understood that SBN obtained by MSS should have larger cell dimensions than that of SBN obtained by CMO.

SEM micrograph of acicular $Sr_{0.4}Ba_{0.6}Nb_2O_6$ particles via MSS is shown in Fig. 2. The synthesised seed particles has the length of 4–43 μm and an aspect ratio of 4–22 (see Table 1).

### 3.2. Effect of $V_2O_5$ on the densification behaviour of textured $Sr_{0.4}Ba_{0.6}Nb_2O_6$ ceramics

The effect of $V_2O_5$ additive on the densification behaviour of $Sr_{0.4}Ba_{0.6}Nb_2O_6$ ceramics is shown in Fig. 3. The density of SBN40 samples increases with sintering temperature whether $V_2O_5$ is added or not. It is noted that the density of $V_2O_5$-free samples increases quickly from 3.45 to 5.18 g/cm$^3$ within a narrow temperature range (1300–1400 °C) and reaches a maximum value at 1425 °C. The addition of $V_2O_5$ helps to improve the densification of SBN40 markedly. For example, even if it is sintered at 1100 °C, the $V_2O_5$-containing sample has a density of 4.38 g/cm$^3$, which is much higher than $V_2O_5$-free sample sintered at 1350 °C (4.07 g/cm$^3$). Thus, $V_2O_5$-containing SBN with relatively higher density can be sintered at lower temperature. It is reported that $V^{5+}$ ions are rarely dissolved in the tungsten bronze structure.[15] Thus, $V_2O_5$ exists as liquid phase in the grain boundaries at not very high temperature because of low melting point (690 °C), promoting the densification of SBN ceramics. With the increase in temperature, the viscosity of molten $V_2O_5$ decreases, which helps $V_2O_5$ to spread out across the grains, and consequently density increases. However, too high a temperature will result in the decrease of density owing to the evaporation of $V_2O_5$.

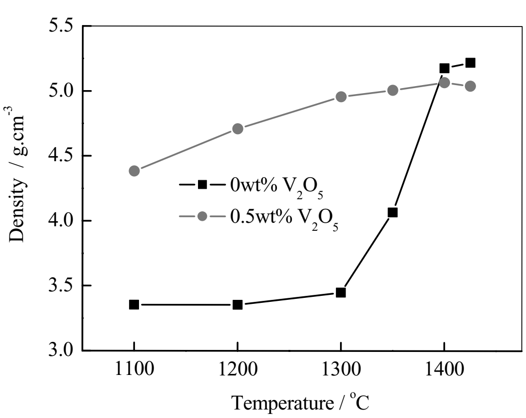


Fig. 3. The effect of $V_2O_5$ on the densification behaviour of $Sr_{0.4}Ba_{0.6}$-$Nb_2O_6$ ceramics.

### 3.3. Effect of $V_2O_5$ on the texture development of $Sr_{0.4}Ba_{0.6}Nb_2O_6$ ceramics

XRD patterns of $V_2O_5$-free SBN samples prepared with seed particles sintered at 1400 and 1425 °C are shown in Fig. 4b and c; the XRD pattern of sample prepared without seeds and $V_2O_5$ is also given for comparison (Fig. 4a). Strong {0 0 *l*} XRD peaks of seed-containing sample do not occur unless the sintering temperature is higher than 1425 °C, indicating that texture development is not easy under the condition of absence of $V_2O_5$. The addition of seed particles makes every peak position turn left slightly, which is probably related to $K^+$ ions in template particles. XRD patterns of $V_2O_5$-containing SBN samples prepared with seed particles, sintered at different temperatures are shown in Fig. 5, as well as that of sample sintered at 1300 °C without seeds. Similar to $V_2O_5$-free samples, the grains in the sample without template particles do not exhibit a preferred orientation (see Fig. 5a). In contrast, the sample prepared with seeds sintered at 1200 °C shows strong {0 0 *l*} peaks in the XRD pattern, suggesting that with the aid of $V_2O_5$ texture begins to develop at lower temperature. With the increase of temperature, the {0 0 *l*} peaks dominate the diffraction pattern for samples sintered above 1300 °C.

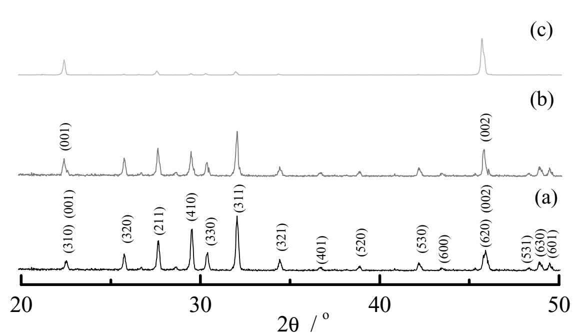


Fig. 4. XRD patterns of $V_2O_5$-free SBN samples prepared without (a) or with seed particles sintered at 1400 °C (b) and 1425 °C (c).

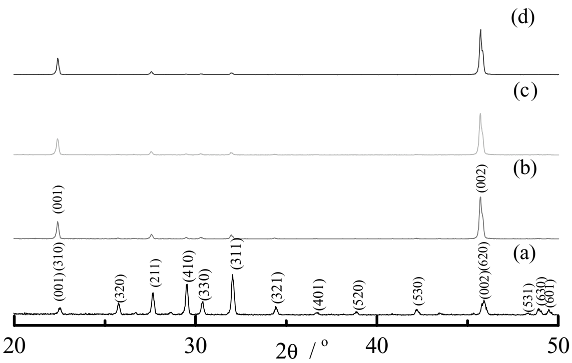


Fig. 5. XRD patterns of $V_2O_5$-containing samples prepared without (a) or with seed particles sintered at 1200 °C (b), 1300 °C (c) and 1400 °C (d).

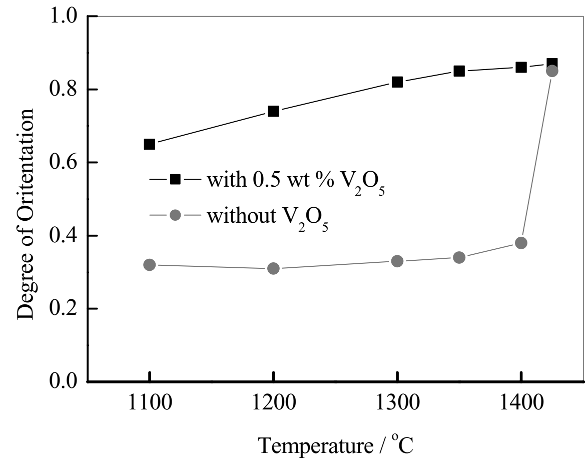


Fig. 6. Degree of orientation as a function of sintering temperature for specimens with and without $V_2O_5$.

The degree of orientation $F_{(00l)}$, was calculated using the following equations (Lotgering method)[16]:

$$F = \frac{P - P_0}{1 - P_0} \quad (1)$$

$$P = \frac{\sum I_{\{00l\}}}{\sum I_{\{hkl\}}} \quad (2)$$

$$P_0 = \frac{\sum I_{0\{00l\}}}{\sum I_{0\{hkl\}}} \quad (3)$$

where $I$ and $I_0$ are the peak intensities of oriented and random samples, $P$ and $P_0$ are the ratio of $\{0\,0\,l\}$ and $\{h\,k\,l\}$ peak intensities in the oriented and random samples, respectively. In this work, the diffraction lines between $2\theta = 20$ and $50°$ were chosen to calculate $P$ and $P_0$.

Fig. 6 shows the effect of $V_2O_5$ on the degree of alignment for the specimens prepared with or without $V_2O_5$ as a function of sintering temperature. It can be seen that degree of orientation in specimens prepared without $V_2O_5$ is small below 1400 °C and quickly reaches a maximum (0.85) at 1425 °C. In contrast, the $V_2O_5$-containing sample sintered at 1100 °C has a high degree of orientation of 0.65, and then the degree of orientation increases gradually with increasing temperature to a maximum of 0.86. These results indicate that the presence of liquid phase $V_2O_5$ favours the formation of textured SBN40 ceramics. For specimens prepared without $V_2O_5$, the rapid growth of seed particles leads to high texture at 1425 °C.

SEM micrographs of samples, parallel to tape casting direction, of $V_2O_5$-containing samples prepared with seeds, sintered between 1200 and 1425 °C have similar microstructures, i.e. some large, highly anisotropic grains are aligned. The microstructure of $V_2O_5$-containing sample sintered at 1200°C is shown in Fig. 7a. Thus, strong morphologic texture can be easily obtained in $V_2O_5$-containing samples by introducing aligned template particles. However, the microstructure of $V_2O_5$-free samples is quite different. Only equi-axed grains can be seen in the sample even though it was sintered at 1425 °C, see Fig. 7b. EDS analysis shows that all the vanadium exist in grain boundaries. Obviously, the differences in microstructure of two samples with and without $V_2O_5$ result from the presence of $V_2O_5$, since $V_2O_5$ with low melting point will become liquid phase during sintering and promote the faster growth of $(0\,0\,l)$ planes having high surface energy.

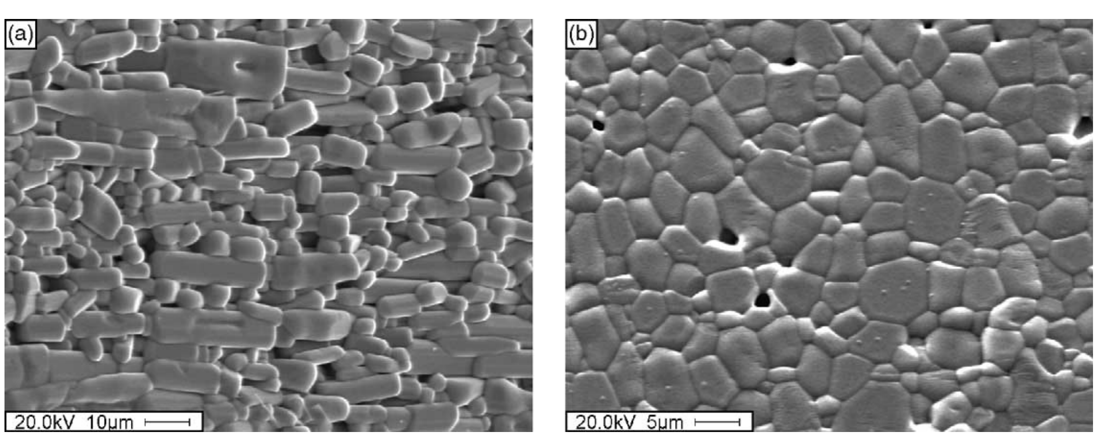


Fig. 7. SEM micrographs of $V_2O_5$-containing sample sintered at 1200 °C (a) and $V_2O_5$-free sample sintered at 1425 °C (b).

Table 2
Comparison of temperature and $V_2O_5$ additive on texture development, dielectric properties of SBN40 sample prepared at different conditions

| Preparation conditions | | | The degree of orientation | $T_c$ (Curie temperature) (°C) | $\varepsilon$ at room temperature | $\varepsilon$ at $T_c$ |
|---|---|---|---|---|---|---|
| Seed particles | $V_2O_5$ | Temperature (°C) | | | | |
| With | With | 1200 | 0.74 | 181 | 487 | 5072 |
| With | With | 1300 | 0.82 | 182 | 553 | 5686 |
| With | With | 1400 | 0.86 | 181 | 581 | 7065 |
| With | Without | 1400 | 0.38 | 181 | 594 | 3412 |
| With | Without | 1425 | 0.81 | 182 | 482 | 5000 |
| Without | Without | 1300 | 0 | 156 | 550 | 1030 |

### 3.4. Effect of $V_2O_5$ on the dielectric properties of textured $Sr_{0.4}Ba_{0.6}Nb_2O_6$ ceramics

Fig. 8 shows the orientation-dependence and temperature dependence of the dielectric constant and dielectric loss at 1 kHz for a $V_2O_5$-containing sample sintered at 1300 °C for 3 h. In Fig. 8a, the dielectric constant at room temperature in the direction perpendicular to the *c*-axis (6 0 7) is higher than the parallel to the *c*-axis (2 4 4), which is consistent with the well-known dielectric anisotropy in single crystals.[17] The anisotropy in the dielectric constant between the perpendicular- and parallel-cut samples increases with increasing temperatures and reaches a maximum at the Curie temperature $T_c$ ($\varepsilon_r = 5686$ and 550, respectively). These two orientations also show different dielectric-loss behaviours, presumably because the electrical conductivity in the parallel cuts is higher than perpendicular cuts.

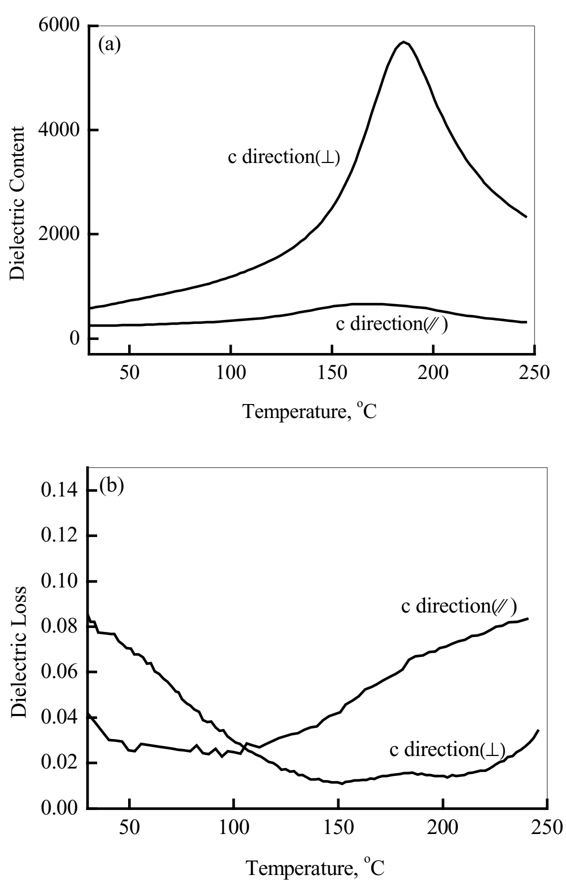


Fig. 8. Temperature and crystallographic direction dependence of the dielectric constant (a) and dielectric loss (b) for $V_2O_5$-containing sample sintered at 1300 °C for 3 h.

Table 2 shows the effect of temperature and $V_2O_5$ additive on dielectric properties of SBN40. Whether $V_2O_5$ is added or not, the samples prepared with seed particles have almost the same $T_c$, indicating that $T_c$ is not influenced by the addition of $V_2O_5$. However, in comparison with the sample prepared without seed particles, the samples prepared with seed particles have higher $T_c$ value, showing that the addition of seed particles influences the $T_c$ of SBN40 value. Previous investigation[18,19] shows that when alkali elements, such as sodium and potassium, are present in the structure, they will partially or fully occupy the interstitial sites with no vacancy left and this causes the value of $T_c$ to increase, which stabilises the ferroelectric structure. From Table 2, $T_c$ of the sample prepared without seed particles and $V_2O_5$ approaches single crystal SBN40 ($T_c$ = 158 °C).[17] In addition, similar to the tendency of degree of orientation versus temperature, $\varepsilon$ at both room temperature and Curie temperature increases with increasing sintering temperature, indicating that the dielectric properties of textured SBN40 ceramics increase with the degree of orientation.

Due to lack of $\varepsilon_r$ of single crystal SBN40, we cannot compare our data with single crystal. But from the above experimental results, it can be seen that the addition of $V_2O_5$ is helpful to improve the degree of orientation and therefore increases the dielectric anisotropy.

## 4. Conclusions

The acicular $Sr_{0.39}Ba_{0.48}K_{0.32}Nb_2O_6$ single crystal particles with the aspect ratio of 4–22 were obtained in molten $K_2SO_4$ salt at 1300 °C for 3 h. By using these single crystal particles as templates, textured $Sr_{0.4}Ba_{0.6}Nb_2O_6$ (SBN40) ceramics were prepared.

The addition of $V_2O_5$ favours the lowering of the sintering temperature of the textured SBN40 ceramics and the growth of seed particles, resulting in the improvement of the degree of orientation and the anisotropy of dielectric properties between perpendicular- and parallel-cut directions in textured SBN40.

## Acknowledgements

This research is supported by the National Natural Science Foundation of China and the Outstanding Overseas Chinese Scholars Fund of Chinese Academy of Science.

## References


1. Antisigin, V. D., Kotsov, E. G., Malinovsky, V. K. and Sterelyukhina, L. N., Electrooptics of thin ferroelectric films. *Ferroelectrics* 1981, **38**, 761–763.
2. Lenzo, P. V., Spencer, E. G. and Ballman, A. A., Electrooptic coefficients of ferroelectric strontium barium niobate. *Appl. Phys. Lett.* 1967, **11**, 23.
3. VanDamme, N. S., Sutherland, A. E., Jones, L., Bridger, K. and Winzer, S. R., Fabrication of optically transparent and electrooptic strontium barium niobate ceramics. *J. Am. Ceram. Soc.* 1991, **74**, 1785–1792.
4. Glass, A. M., Investigation of $Sr_{1-x}Ba_xNb_2O_6$ with special reference to pyroelectric detection. *J. Appl. Phys.* 1969, **40**, 4699–4713.
5. Lee, S. I. and Choo, W. K., Modified ferroelectric high-density strontium barium niobate ceramics for pyroelectric applications. *Ferroelectrics* 1988, **87**, 209–212.
6. Neurgaonkar, R. R., Kalisher, M. H., Lim, T. C., Staples, E. J. and Keester, K. I., Piezoelectric tungsten bronze crystals for SAW device applications. *Mater. Res. Bull.* 1980, **15**, 1235.
7. Moreno-Gobbi, A., Pérez, M., Paolini, G., Negreira, C. A., Garcíra, D. and Eiras, J. A., Ultrasound studies of phase transitions in tungsten bronze ferroelectric materials. *J. Alloys Comp.* 2000, **310**, 29–31.
8. Duran, C., McKinstry, S. T. and Messing, G. L., Dielectric and piezoelectric properties of textured $Sr_{0.53}Ba_{0.47}Nb_2O_6$ ceramics by templated grain growth. *J. Mater. Res.* 2002, **17**, 2399–2409.
9. Neurgaonkar, R. R. and Cory, W. K., Progress in photorefractive tungsten bronze crystals. *J. Opt. Soc. Am.* 1986, **B3**, 274–282.
10. Neurgaonkar, R. R., Cory, W. K., Oliver, J. R., Ewbank, M. D. and Hall, W. F., Development and modification of photorefractive properties in the tungsten bronze family crystals. *Opt. Eng.* 1987, **26**, 392–405.
11. Woike, T., Dörfler, U., Tsankov, L., Weckwerth, G., Wolf, D., Wöhlecke, M. *et al.*, Photorefractive properties of Cr-doped $Sr_{0.61}Ba_{0.39}Nb_2O_6$ related to crystal purity and doping concentration. *Appl. Phys.* 2001, **B72**, 661–666.
12. Duran, C., McKinstry, S. T. and Messing, G. L., Fabrication and electrical properties of textured $Sr_{0.53}Ba_{0.47}Nb_2O_6$ ceramics by templated grain growth. *J. Am. Ceram. Soc.* 2001, **83**, 2203–2213.
13. Huang, Q. W., Wang, P. L., Cheng, Y. B. and Yan, D. S., XRD analysis of formation of strontium barium niobate phase. *Mater. Lett.* 2002, **56**, 915–920.
14. Jamiesion, P. B., Abrahams, S. C. and Bernstein, J. L., Ferroelectric tungsten bronze-type crystal structures: I. Barium strontium $Ba_{0.27}Sr_{0.75}Nb_2O_{5.78}$. *J. Chem. Phys.* 1968, **48**, 5048–5055.
15. Nishiwaki, S., Takahashi, J. and Kodaira, K., Synthesis and phase transition of ferroelectric $Sr_{0.2}Ba_{0.8}Nb_2O_6$. *J. Ceram. Soc. Jpn., Int. Ed.* 1996, **104**, 413–415.
16. Lotgering, F. K., Topotactical reaction with ferromagnetic oxides having hexagonal crystal structures I. *J. Inorg. Nucl. Chem.* 1959, **9**, 113–123.
17. Neurgaonkar, R. R., Hall, W. F., Oliver, J. R., Ho, W. W. and Copy, W. K., Tungsten bronze $Sr_{1-x}Ba_xNb_2O_6$: a case history of versatility. *Ferroelectrics* 1988, **87**, 167–179.
18. Umakantham, K., Murty, S. N., Rao, K. S. and Bhanumathi, A., Effect of rare-earth ions on the properties of modified SBN ceramics. *J. Mater. Sci. Lett.* 1987, **6**, 565–568.
19. Murty, S. N., Murty, K. V. R., Mouli, K. C., Bhanumathi, A., Raju, S. B., Padmavathi, G. *et al.*, Relaxor behavior in certain tungsten bronze ceramics. *Ferroelectrics* 1994, **158**, 325.